Impedance Characteristics of Quantum-Well Lasers

S. Weisser, I. Esquivias, P. J. Tasker, J. D. Ralston, *Member, IEEE*, B. Romero, and J. Rosenzweig

***Abstract*—We derive theoretical expressions for the impedance of quantum-well lasers below and above threshold based on a simple rate equation model. These *electrical* laser characteristics are shown to be dominated by purely *electrical* parameters related to carrier capture/transport and carrier re-emission. The results of on-wafer measurements of the impedance of high-speed $In_{0.35}Ga_{0.65}As$/GaAs multiple-quantum-well lasers are shown to be in good agreement with this simple model, allowing us to extract the effective carrier escape time and the effective carrier lifetime, and to estimate the effective carrier capture/transport time.**

I. Introduction

SEVERAL models have been proposed to account for the influence of carrier transport, carrier capture and carrier re-emission on the dynamic properties of quantum-well (QW) lasers [1]–[4]. These models typically consider the interplay between unconfined carriers in the core region and confined carriers in the quantum wells (QW's) by means of an effective carrier capture/transport time, τ_{cap}, and an effective carrier escape time, τ_{esc}. The determination of these time constants *under the operating conditions of interest* is thus of maximum interest in order to optimize the high-speed performance of QW lasers.

Kan and Lau have proposed an electrical equivalent circuit for QW lasers [5], and have demonstrated that the electrical impedance is very sensitive to the values of τ_{cap} and τ_{esc}. We have recently presented impedance and modulation response measurements of p-doped $In_{0.35}Ga_{0.65}As$/GaAs multiple quantum well (MQW) lasers [6]. The impedance characteristics of these devices can be described by a simple RC circuit, with a bias-dependent time constant, τ_0, which takes into account the combined influence of τ_{cap} and of the space-charge capacitance, C_{sc}. In these highly-doped lasers, the following conditions explain the observed behaviour of the impedance: i) $\tau_{\text{cap}}/\tau_{\text{esc}} \ll 1$, and ii)$\tau_{\text{eff}}/\tau_{\text{esc}} \ll 1$, where τ_{eff} denotes the effective carrier lifetime in the QW's.

In the present work, we derive the theoretical expressions for the differential diode resistance and the frequency-dependent impedance of QW lasers based on a simple model using three rate equations. We compare the model predictions to the experimental values of the impedance of lasers with intentionally undoped $In_{0.35}Ga_{0.65}As$/GaAs MQW active regions, in which the above condition i) is also fulfilled, while condition ii) is no longer valid. The latter gives rise to a distinctly different behaviour of both the frequency-dependent impedance and the differential diode resistance of the undoped devices, as compared to the lasers with p-doped active layers. The results of the measurements are shown to be in good agreement with the theoretical predictions, suggesting that impedance measurements can indeed be a valuable tool with which to directly extract carrier capture/transport parameters.

Manuscript received July 18, 1994; revised September 7, 1994. This work was supported in part by the Bundesministerium für Forschung und Technologie. The work of I. Esquivias and B. Romero was supported by Comisión Interministerial de Ciencia y Tecnología (Spain), Project TIC93-0744-C04-04.

S. Weisser, P. J. Tasker, J. D. Ralston, and J. Rosenzweig are with the Fraunhofer-Institut für Angewandte Festkörperphysik, Tullastraße 72, D-79108 Freiburg, Germany.

I. Esquivias and B. Romero are with the Dept. Tecnología Electrónica, Universidad Politécnica de Madrid, Ciudad Universitaria, E-28040 Madrid, Spain.

IEEE Log Number 9406589.

II. Rate Equations

Neglecting electrical parasitics and recombination of carriers in the core region, the dynamic behaviour of a quantum-well laser is modelled using three rate equations, one each for the volumetric photon density in the cavity, S, the number of unconfined carriers in the core, N_c, and the number of confined carriers in the QW, N_w:

$$\begin{aligned}\frac{dS}{dt} &= S(\Gamma G - 1/\tau_p)\\ \frac{dN_w}{dt} &= -N_w(1/\tau_{\text{eff}} + 1/\tau_{\text{esc}}) + N_c/\tau_{\text{cap}} - SV_{qw}G \quad (1)\\ \frac{dN_c}{dt} &= I/q - \frac{dV_c}{dt}\frac{C_{\text{sc}}}{q} - N_c/\tau_{\text{cap}} + N_w/\tau_{\text{esc}}.\end{aligned}$$

In (1) τ_p denotes the photon lifetime, Γ the confinement factor, $G(N_w, S)$ the material gain, I the injection current, V_c the voltage applied across the core, V_{qw} the QW volume, and q the elementary charge. The material gain is written as $G(N_w, S) = G(N_w)(1 - \varepsilon S)$ with the nonlinear gain coefficient, ε. The influence of the space-charge capacitance, C_{sc}, must be considered in order to properly describe the dynamical characteristics of QW lasers, as is also the case for bulk lasers [7]. It should be noted that τ_{cap} must be interpreted as an *effective* capture time, taking into account both the transport of carriers across the core region and the quantum capture process [8].

III. Differential Diode Resistance

The static solution (N_{w0}, N_{c0}, S_0 etc.) of (1) is obtained by setting the time derivatives to zero, yielding in the case of $\varepsilon \cdot S_0 \ll 1$

$$N_{w0} = \frac{I_0\tau_{\text{eff}}}{q} \text{ and } N_{c0} = \frac{I_0\tau_{\text{cap}}}{q}\left(1 + \frac{\tau_{\text{eff}}}{\tau_{\text{esc}}}\right) \quad (2)$$

1041-1135/94$04.00 © 1994 IEEE

in the subthreshold regime and

$$N_{w0} = N_{w,\mathrm{th}} \text{ and } N_{c0} = \frac{\left(I_0 + \frac{\tau_{\mathrm{eff}}}{\tau_{\mathrm{esc}}} I_{\mathrm{th}}\right)\tau_{\mathrm{cap}}}{q} \quad (3)$$

above threshold, where $I_{\mathrm{th}} = qN_{w,\mathrm{th}}/\tau_{\mathrm{eff}}$ and $N_{w,\mathrm{th}}$ denote the threshold current and the threshold carrier number in the QW, respectively. Above threshold, the material gain is clamped to its threshold value, resulting in a clamping of the carrier number *in the* QW to $N_{w,\mathrm{th}}$ [9].

A key step in the derivation of the differential diode resistance is to relate the carrier number in the core to the voltage applied across the core, V_c. Neglecting electrical parasitics, this relation is expressed as

$$N_c \propto e^{\frac{V_c}{mV_T}} \text{ with } V_T = kT/q, \quad (4)$$

where m, k, and T are the diode ideality factor, the Boltzmann constant, and the absolute temperature, respectively. The differential diode resistance, $R_d = dV_{c0}/dI_0$ is then derived by inserting (4) in (2) and (3) and subsequent differentiation, yielding

$$R_d(I_0) = \begin{cases} \frac{mV_T}{I_0} & \text{for } I_0 < I_{\mathrm{th}} \\ \frac{mV_T}{I_0 + \frac{\tau_{\mathrm{eff}}}{\tau_{\mathrm{esc}}} I_{\mathrm{th}}} & \text{for } I_0 > I_{\mathrm{th}} \end{cases}. \quad (5)$$

(5) predicts a drop in the differential diode resistance at lasing threshold

$$\frac{R_d(I_0 \to I_{\mathrm{th}}, I_0 < I_{\mathrm{th}})}{R_d(I_0 \to I_{\mathrm{th}}, I_0 > I_{\mathrm{th}})} = 1 + \frac{\tau_{\mathrm{eff}}}{\tau_{\mathrm{esc}}} \quad (6)$$

which can be used to estimate the ratio $\tau_{\mathrm{eff}}/\tau_{\mathrm{esc}}$. In the case of *negligible carrier re-emission* $\tau_{\mathrm{eff}}/\tau_{\mathrm{esc}} \ll 1$ (5) simplifies to the corresponding expression for conventional diodes $R_d = mV_T/I_0$, both below and above threshold. Note that R_d does not vanish above threshold, contrary to the behaviour in ideal bulk lasers [10]. In general, the terminal voltage in QW lasers is not clamped above threshold, because the carrier number *in the core* increases even above threshold, as can be seen from (3).

IV. Frequency-Dependent Impedance

The solution of (1) in the small-signal regime is obtained by expanding the variables I, S, N_w, and N_c around their steady-state values, e.g., $S(t) = S_0 + s(\omega)e^{j\omega t}$. We further introduce the relaxation frequency, $\omega_r = \sqrt{G' S_0/\tau_p}$ with the differential gain, $G' = V_{qw}\partial G/\partial N_w$, the damping rate, $\gamma = 1/\tau_{\mathrm{eff}} + \omega_r^2(\tau_p + \varepsilon/G')$, and the bias-dependent electrical diode time constant

$$\tau_0(I_0) = \tau_{\mathrm{cap}} + \xi \cdot R_d(I_0) \cdot C_{\mathrm{sc}}(I_0) \quad (7)$$

with $\xi = \tau_{\mathrm{esc}}/(\tau_{\mathrm{eff}} + \tau_{\mathrm{esc}})$ below threshold and $\xi = 1$ above threshold. Note that there is no discontinuity in τ_0 at threshold, as can be seen from (5) and (7). The electrical diode time constant summarizes the effects of charge stored in the core and of charge stored in the depletion region of the p-n junction.

Using (4) and (5) in conjunction with this small-signal solution, the exact expression for the frequency-dependent impedance, $Z(\omega) = v_c(\omega)/i(\omega)$, can be derived. This exact expression, however, is quite lengthy and its physical interpretation is therefore difficult. In the limit of *weak carrier re-emission*, $\tau_0/\tau_{\mathrm{esc}} \ll 1$ and $\varepsilon \cdot S_0 \ll 1$, this expression simplifies to

$$Z(\omega) = R_d \frac{1}{1 + j\omega\tau_0} T(\omega) \quad (8)$$

with the function $T(\omega)$ given by

$$T(\omega) = \frac{1 + j\omega\tau_1}{1 + j\omega\tau_{\mathrm{eff}}} \text{ with } 1/\tau_1 = 1/\tau_{\mathrm{eff}} + 1/\tau_{\mathrm{esc}} \quad (9)$$

in the subthreshold regime and by the expression

$$T(\omega) = \frac{\omega_r^2 - \omega^2 + j\omega\gamma_I}{\omega_r^2 - \omega^2 + j\omega\gamma} \text{ with } \gamma_I = \gamma + 1/\tau_{\mathrm{esc}} \quad (10)$$

above threshold.

Below threshold, (8) and (9) predict an impedance function with two poles and one zero. Above threshold, $T(\omega) = 1$ both at very low ($\omega \ll \omega_r$) and at very high frequencies ($\omega \gg \omega_r$). Equations. (8) and (10) then predict a peak in the impedance at the relaxation frequency with the relative magnitude $T(\omega_r)/T(0) = \gamma_I/\gamma$ if $\tau_0\omega_r \ll 1$. At high bias currents, $\gamma_I \approx \gamma$, and the peak in the impedance disappears. In the case of *negligible carrier re-emission* $\tau_{\mathrm{eff}}/\tau_{\mathrm{esc}} \ll 1$, the relations $\tau_I = \tau_{\mathrm{eff}}$ and $\gamma_I = \gamma$ hold, and thus $T(\omega) = 1$, both below and above threshold. The impedance in this case simplifies for all bias currents to the impedance of a simple RC parallel circuit with the time constant τ_0.

V. Measurements

In order to investigate the validity of the above model, we performed on-wafer measurements of the differential diode resistance and the frequency-dependent impedance of MBE-grown, high-speed $In_{0.35}Ga_{0.65}As/GaAs$ MQW lasers with undoped active regions. The lasers were fabricated in a triple-mesa structure with an active mesa width of 3 μm and a cavity length of 200 μm. Further details of the epilayer sequence and the lateral device structure are reported in [11]. The differential diode resistance was determined by numerical differentiation of the DC current-voltage characteristics measured using a HP 4145 semiconductor parameter analyzer. On-wafer measurements of both magnitude and phase of the frequency-dependent impedance were performed using a fully calibrated HP 8722A network analyzer.

In order to properly model the measured values of the impedance, a parasitic series resistance R_s has to be added to the impedance derived from the rate equations. Fig. 1 presents $I_0\frac{dV_0}{dI_0} = I_0(R_d + R_s)$, where $V_0 = V_{c0} + I_0 \cdot R_s$ is the terminal voltage, as a function of I_0, demonstrating the drop in R_d at threshold predicted by (6). After correcting for the effect of the series resistance, the measured values of $I_0\frac{dV_0}{dI_0}$ slightly below and above threshold can be further used to estimate $\tau_{\mathrm{eff}}/\tau_{\mathrm{esc}}$ at threshold using (6), yielding $\tau_{\mathrm{eff}}/\tau_{\mathrm{esc}} \approx 0.8$.

Fig. 2 presents the measured magnitude of the frequency-dependent impedance, Mag(Z), versus frequency for various bias currents in the vicinity of threshold. Below threshold, the curves demonstrate the behaviour predicted by (8) and (9)

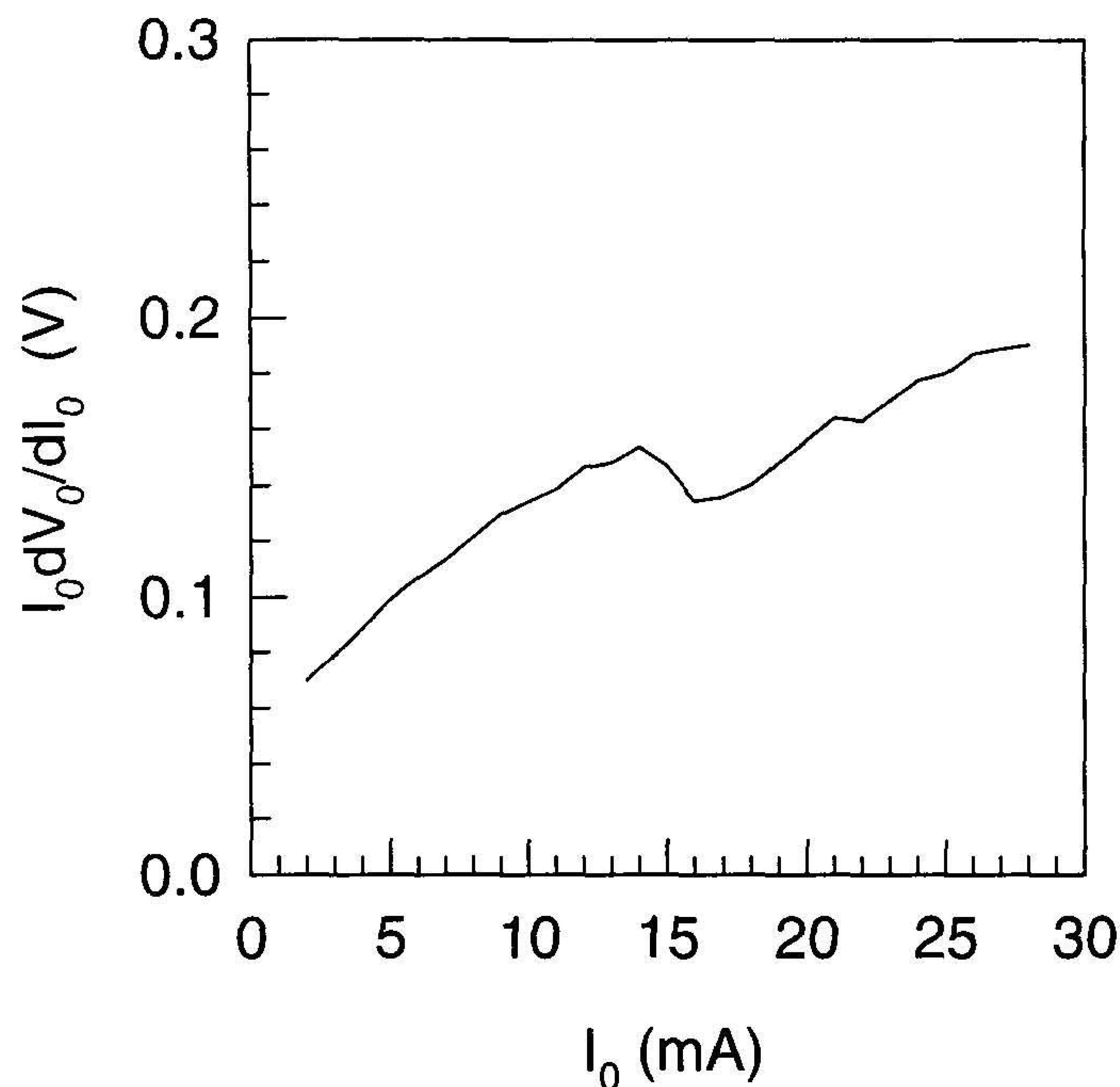

Fig. 1. Measured differential diode resistance of a 3 × 200 μm^2 laser with four undoped $In_{0.35}Ga_{0.65}As/GaAs$ QW's versus bias current, I_0. The threshold current is 14.5 mA.

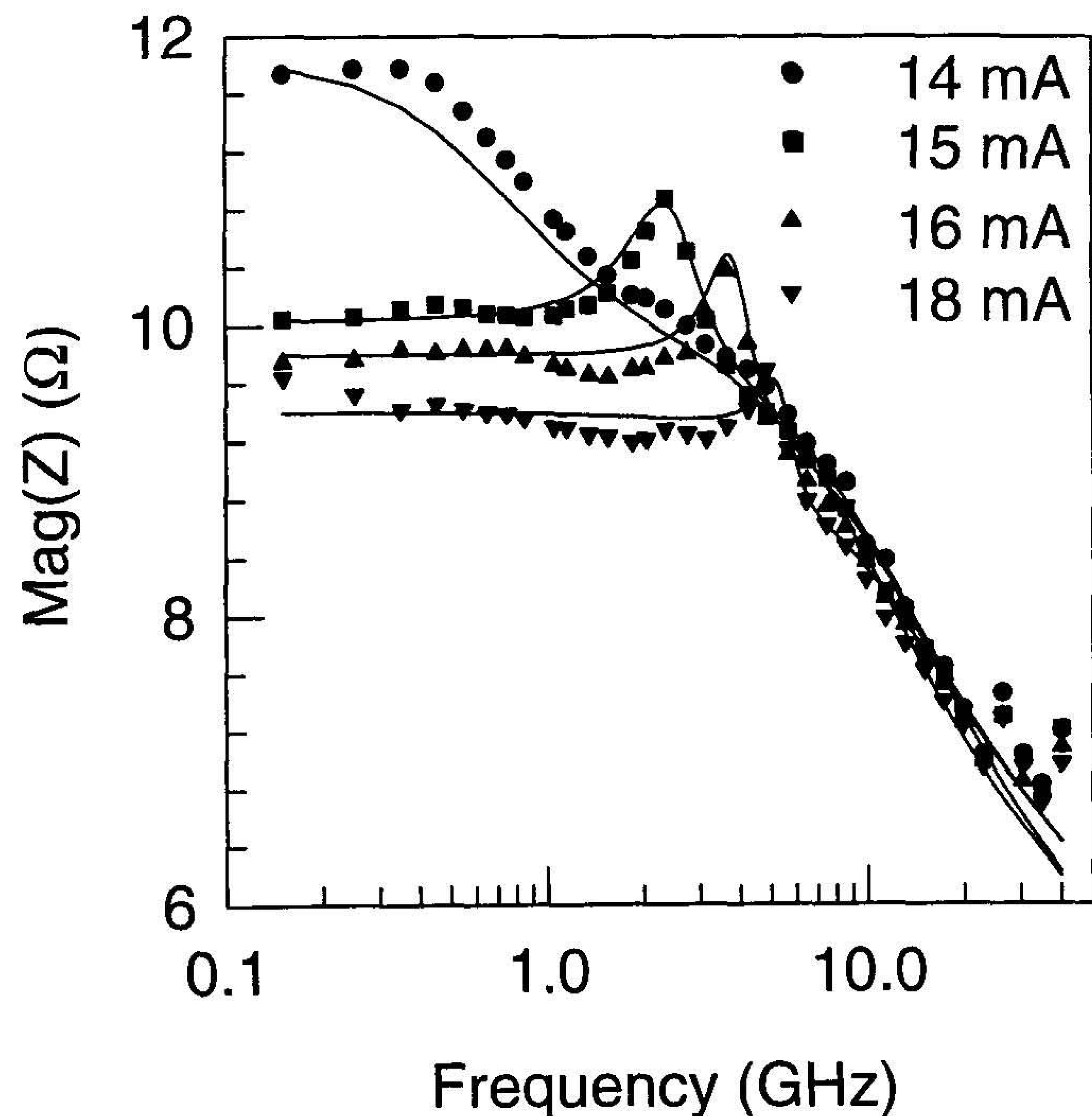

Fig. 2. Measured and fitted (see text) impedance of a 3 × 200 μm^2 laser with four undoped $In_{0.35}Ga_{0.65}As/GaAs$ QW's versus frequency at various bias currents in the vicinity of the lasing threshold.

with two poles and one zero. This figure further demonstrates that the differential diode resistance does not vanish above threshold, in agreement with (5). Above threshold, the low-frequency pole disappears and a peak in the impedance is observed at the relaxation frequency. By fitting both the magnitude and the phase of the *exact* small-signal solution of (1)–(3) to the experimental results (see fit curves in Fig. 2), we were able to extract the values of τ_0, $\tau_{\rm eff}$, and $\tau_{\rm esc}$ as a function of the bias current. At threshold, $\tau_{\rm eff}$ and $\tau_{\rm esc}$ are found to be 0.3 and 0.45 ns, respectively, which is consistent with the ratio $\tau_{\rm eff}/\tau_{\rm esc}$ extracted from the drop in R_d. The electrical time constant τ_0, is found to decrease with increasing bias current from 30 ps at 1 mA bias to approximately 10 ps at bias currents well above threshold, yielding a ratio $\tau_0/\tau_{\rm esc}$ below 0.1 and justifying the approximation made in the derivation of (9)–(11). From (7), the above results also yield an upper limit of 10 ps for the effective carrier capture time, $\tau_{\rm cap}$, at high bias currents.

VI. Conclusion

In summary, we have derived the theoretical expressions for the impedance of QW lasers using a simple rate equation model. By fitting the theoretical expressions to the results of on-wafer measurements of the impedance of $In_{0.35}Ga_{0.65}As/GaAs$ MQW lasers with undoped active regions, the effective carrier escape time, the effective carrier lifetime in the QW's, and the electrical diode time constant could be extracted.

Acknowledgment

The authors wish to thank W. Benz, J. Fleissner, E. C. Larkins, B. Matthes, K. Bender and A. Schönfelder for their assistance with sample preparation and characterization. We also wish to thank G. Grau and H. Rupprecht for their continuing support and encouragement.

References

[1] M. O. Vassell, W. F. Sharfin, W. C. Rideout, and J. Lee, "Competing effects of well-barrier hole burning and nonlinear gain on the resonance characteristics of quantum-well lasers," *IEEE J. Quantum Electron.*, vol. 29, pp. 1319–1329, 1993.

[2] T. C. Wu, S. C. Kan, D. Vassilovski, K. Y. Lau, C. E. Zah, B. Pathak, and T. P. Lee, "Gain compression in tensile strained 1.55 μm quantum well lasers operating at first and second quantized states," *Appl. Phys. Lett.*, vol. 60, pp. 1794–1796, 1992.

[3] R. Nagarajan, M. Ishikawa, T. Fukushima, R. S. Geels, and J. E. Bowers, "High speed quantum-well lasers and carrier transport effects," *IEEE J. Quantum Electron.*, vol. 28, pp. 1990–2008, 1992.

[4] N. Tessler, R. Nagar, and G. Eisenstein, "Structure dependent modulation responses in quantum-well lasers," *IEEE J. Quantum Electron.*, vol. 28, pp. 2242–2250, 1992.

[5] S. C. Kan and K. Y. Lau, "Intrinsic equivalent circuit of quantum-well lasers," *IEEE Photon. Technol. Lett.*, vol. 4, pp. 528–530, 1992.

[6] S. Weisser, I. Esquivias, P. J. Tasker, J. D. Ralston, and J. Rosenzweig, "Impedance, modulation response, and equivalent circuit of ultra-high-speed $In_{0.35}Ga_{0.65}As/GaAs$ MQW lasers with p-doping," *IEEE Photon. Technol. Lett.*, vol. 6, no. 4, pp. 782–785, 1994.

[7] R. S. Tucker and D. J. Pope, "Microwave circuit models of semiconductor injection lasers," *IEEE Trans. Microwave Theory Technol.*, vol. 31, pp. 289–294, 1983.

[8] S. C. Kan, D. Vassilovski, T. C. Wu, and K. Y. Lau, "Quantum capture limited modulation bandwidth of quantum well, wire, and dot lasers," *Appl. Phys. Lett.*, vol. 62, pp. 2307–2309, 1993.

[9] Ch. S. Harder, B. J. Van Zeghbroeck, M. P. Kesler, H. P. Meier, P. Vettiger, D. J. Webb, and P. Wolf, "High-speed GaAs/AlGaAs optoelectronic devices for computer applications," *IBM J. Res. Develop.*, vol. 34, pp. 568–583, 1990.

[10] W. B. Joyce and R. W. Dixon, "Electrical characterization of heterostructure lasers," *J. Appl. Phys.*, vol. 49, pp. 3719–3728, 1978.

[11] J. D. Ralston, S. Weisser, I. Esquivias, E. C. Larkins, J. Rosenzweig, P. J. Tasker, and J. Fleissner, "Control of differential gain, nonlinear gain, and damping factor for high-speed applications of GaAs-based MQW lasers," *IEEE J. Quantum Electron.*, vol. 29, pp. 1648-1659, 1993.